Cultivated Land Information Extraction and Spatial Pattern Analysis in Beijing Based on Deep Learning

Zitong Yan[1,2], Hao Wu[1], Jun Zhang[1], Dongyang Hou[3]

[1] National Geomatics Center of China, Beijing, China, 100830 - yzt921@qq.com, (wuhao, junzhang)@ngcc.cn
[2] China University of Mining & Technology (Beijing), Beijing, China, 100083 - yzt921@qq.com
[3] School of Geoscience and Information Physics, Central South University, Changsha, China, 410083 - houdongyang1986@csu.edu.cn

Keywords: Cultivated land; Spatial pattern; HRNet; Information extraction; Fragmentation.

Abstract

Cultivated land is the basic resource and material condition for human survival, providing the necessary material basis for agricultural development and agricultural modernization (Tian and Shi, 2024). For this reason, this paper takes Beijing as an experimental area to study the cultivated land extraction method and analyze the distribution pattern of cultivated land and the degree of fragmentation. The results show that (1) the extraction results are evaluated by using confusion matrix and Kappa coefficient, and the Kappa coefficient is obtained to be 0.8358.(2) The cultivated land in Beijing is mainly distributed in the southeast as well as the northwest of the local area of gentle terrain, and the The range of the extremely high value of cultivated land kernel density in 2017-2022 is significantly reduced, the slope of the area with the smallest reduction in the proportion of cultivated land is less than 5°, the reduction in the area of cultivated land in water resource-rich areas is small, and the reduction in the proportion of cultivated land in road-intensive areas is large. (3) Due to various natural factors and human activities, the degree of cultivated land fragmentation in Beijing is increasing, the boundary shape of cultivated land patches tends to be irregular.

1. Introduction

Cultivated land is vital for agriculture, rural areas, and farmer well-being, impacting both national economy and people's livelihoods (Huang et al., 2019). Remote sensing technology offers distinct advantages for large-scale cultivated land studies. Its synchronous, large-area observation capabilities and high timeliness provide rich data for extraction and spatial pattern analysis. Remote sensing images can capture the complex and diverse shapes of cultivated land. Deep learning methods, particularly target detection and semantic segmentation, excel at extracting features and determining the spatial location and category of each land element (Cheng et al., 2017). The spatial pattern of cultivated land refers to its distribution and configuration. Its formation is influenced by both the inherent characteristics of the land itself and the surrounding natural and socio-economic environment (Brabec and Smith, 2002). Researching this spatial pattern, including its formation mechanisms and the interplay between land, environment, and socio-economic factors, allows for predictions and effective management of future land patterns. This holds significant theoretical and practical value for comprehensive cultivated land improvement and agricultural modernization (Geng et al., 2021).

2. Study area and data

2.1 Study area

Beijing is located in the northern part of the North China Plain, adjacent to Bohai Bay and Tianjin. The terrain is high in the northwest and gently slopes down to plains in the southeast, with an average elevation of 43.5 m (Qiu et al., 2021). The area is rich in water resources, including rivers, lakes and reservoirs. In general, Beijing's topography, climate, hydrology, and other natural geographic conditions are favourable for agricultural development, with wheat and corn being the main crops (Yin et al., 2024).

However, due to Beijing's unique position as the "capital city", population growth and rapid urban expansion have led to a steady decline in the food production capacity of cultivated land. Large tracts of continuous farmland land have been fragmented, and clear boundaries between cultivated land and urban areas have become increasingly blurred (Yin et al., 2019). This has exacerbated the issues facing cultivated land, significantly hindering agricultural development.

2.2 Data source and sample set production

In this study, the Google Earth Engine remote sensing cloud computing platform was utilized to acquire Sentinel-2A image data of the Beijing area from September 2017 and September 2022. These images contain three visible bands-red, green, and blue-with a spatial resolution of 10 meters. These datasets are widely used for remote sensing image classification. Additionally, clouds in Sentinel-2 images can be quickly removed using the QA bands provided officially, and the cloud-free areas are processed by overlaying images from different time periods (Cai et al., 2019). For this study, the area was categorized into two land classes: cultivated land and non-cultivated land. Cultivated land samples were manually annotated with reference to Google map images from both 2017 and 2022 to create the label file. The large remote sensing images were then cropped into smaller images of 256 px*256 px with a cropping step of 64 px. Data enhancement methods such as rotation and flipping were applied to generate 3,544 images and their corresponding labels. These images were randomly divided into a training set and validation set in a 7:3 ratio.

Furthermore, auxiliary data such as Beijing's 90m DEM data, township and street-level administrative planning data, water system data, and OpenStreetMap road network data were used

for landscape pattern analysis. This auxiliary data forms a reliable database for this study.

3. Methodology

In this study, we addressed the national demand for cultivated land protection by focusing on Beijing as our study area. We created a sample set of cultivated land to train a deep learning network to extract cultivated land patches. Using HRNet, we set relevant parameters to pre-train the model, and adjusted these parameters multiple times to select the model with the best training results based on accuracy, recall and other indicators. Once the model was trained, we used it to extract cultivated land from the remote sensing image data of Beijing. We then compared the extracted cultivated land with actual labels and calculated evaluation indexes such as the Kappa coefficient to assess the cultivated land extraction results. Finally, we conducted a landscape pattern analysis of the cultivated land. This analysis included examining the distribution of cultivated land, trends in cultivated land change, driving factors, fragmentation, and spatial agglomeration characteristics of cultivated land fragmentation. The goal was to provide a theoretical and practical basis for the country to rationalize the layout of cultivated land, improve its quality, and implement effective cultivated land protection policies.

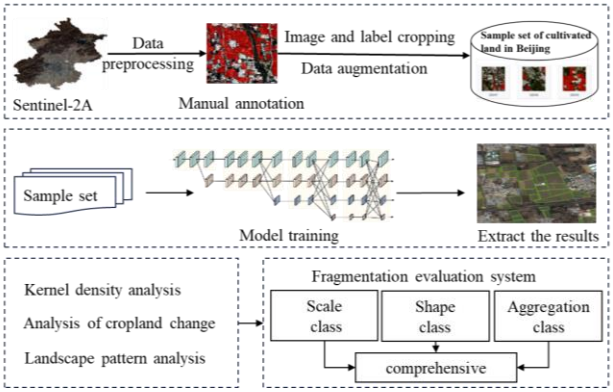

Figure 1. Research framework of cultivated land extraction and spatial pattern analysis.

3.1 Cultivated land extraction

HRNet (High-Resolution Network) is a deep convolutional neural network designed to efficiently process high-resolution images and provide accurate prediction results (Zhu et al., 2019). The overall structure of HRNet is shown below. In this structure, the horizontal direction indicates the depth of the network, while the vertical direction represents the scale of the feature map.At each stage of the network, a new branch is added with half the resolution and double the number of channels, running in parallel with the original channels. This architecture allows for the effective fusion of multi-scale information by exchanging information across parallel multi-resolution sub-networks at different stages (Akhyar et al., 2024). This design enables HRNet to consistently provide robust semantic information and precise positional information, making it particularly well-suited for location-sensitive tasks such as object detection and semantic segmentation.

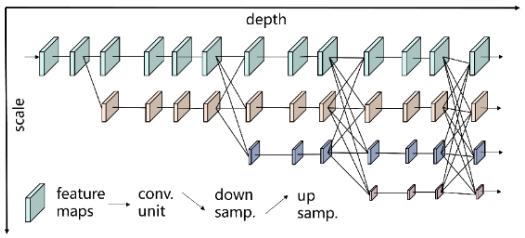

Figure 2. HRNet frame diagram.

HRNet's fusion module ensures that the output of each stage is the result of fusing information from parallel tributaries (Zhao et al., 2023). Taking the fusion module for four representations as an example, each output is the result of summing the four input representations after transforming them by a conversion function, calculated as:

$$R_r^o = f_{1r}(R_1^i) + f_{2r}(R_2^i) + f_{3r}(R_3^i) + f_{4r}(R_4^i) \qquad (1)$$

Where f_{xr} (R) = the conversion function.
x = the xth input
r = the rth output.

When x=r, no conversion is performed on the representation, when x<r, downsampling is performed, and when x>r, upsampling is performed to increase the resolution.

In this study, cultivated land extraction is considered as a binary classification problem, dividing the study area into cultivated land and non-cultivated land categories. Cultivated land was manually labeled in Sentinel-2 imagery from 2017 and 2022, using Google imagery as a reference. A sample set of cultivated land was created by randomly selecting areas and cropping the cultivated land vector labels and images. To increase the number of samples and prevent overfitting during training data augmentation techniques were employed to expand sample set. The datasets was then randomly divided into a training set and a validation set in a 7:3 ratio. The training set was used to train the HRnet deep learning network, while the validation set was used to evaluate the trained model for cultivated land extraction. The model parameters were continuously adjusted to select the model with the best performance. The optimized model was then applied to the entire Beijing area to extract cultivated land (Li et al., 2021)

Parameter	1	3	4	5
Initial learning rate	0.00001	0.00001	0.00001	0.00001
Class weight	1:1	1:4	4:1	10:1
Area weight	1:1	1:1	1:1	1:1
Loss	2.258	2.212	2.168	2.318
IoU	0.816	0.785	0.801	0.835
Recall	0.845	0.864	0.898	0.718
Precision	0.811	0.778	0.894	0.934
Accuracy	0.884	0.855	0.976	0.869
F1	0.826	0.805	0.890	0.754

Table 1. Model training parameters.

The table presents the main parameters involved in the debugging process, as well as some records of the training indices corresponding to the obtained model. After repeated training, a training batch size of 3000 and a cropping size of 468 px were selected as the most appropriate. The debugging mainly

focused on adjusting the initial learning rate, category weights, and area weights to observe the effects of these parameters on the model's training indices. The final selected model achieved a recall of 89.8%, an accuracy of 97.6%, a precision of 89.4%, and an F1 score of 0.89. The initial learning rate for this model was set to 0.00001, and the category weights were set to 4:1.

3.2 Analysis of spatial patterns

3.2.1 Landscape pattern index: Landscape pattern typically refers to the spatial layout of the landscape, encompassing both the distribution and arrangement of landscape elements of various shapes and sizes on the surface, as well as the reflection of landscape heterogeneity(Liu et al., 2021). The landscape pattern index serves not only as a quantitative indicator of landscape structure, but also as a comprehensive summary of landscape pattern information (Wahyudi et al., 2019). Changes in these indices can quantitatively reflect shifts in land use patterns across various dimensions.

Based on existing studies, 12 indices suitable for analyzing the landscape pattern of cultivated land in Beijing were selected according to the distribution characteristics of cultivated land in the area (Chen et al., 2019). Calculations were performed using Fragstats software, which enabled the computation and analysis of the landscape pattern indices and the changes in characteristics of Beijing's cultivated land for the years 2017 and 2022. These indices include 9 class-level indices and 3 landscape-level indices, as shown in the following table.

Landscape pattern index	Units	Description
NP	a	Represents the total number of plots of cultivated land in the study area
PD	a/km²	Represents the number of map spots in the unit area of cultivated land.
AI	%	Indicates the degree of separation between different plots of cultivated land.
LPI	%	Indicates the dominant pattern in the landscape
LSI	/	The larger the index, the more irregular the shape of cultivated land pattern.
AREA_AM	km²	The smaller the value, the greater the degree of cultivated land fragmentation.
SHAPE_AM	/	This value is used to describe the regularity of the overall shape of cultivated land pattern
CLUMPY	%	This value can reflect the aggregation degree and dispersion state of cultivated land pattern spots in the landscape.
DIVISION	/	This value indicates the degree of separation between different plots of cultivated land.

Table 2. Landscape pattern index at class scale.

Landscape pattern index	Units	Description
ED	m/km²	This value indicates the degree to which a landscape or type is divided by a boundary.
FRAC_MN	/	This value is the average value of the sum of the fractal dimensions of each spot in the landscape
CONTAG	%	This value can reflect the aggregation degree or spreading trend of different pattern types in the landscape.

Table 3. Landscape pattern index at landscape scale.

3.2.2 Cultivated land Fragmentation : The study of cultivated land fragmentation can draw on research methods and ideas from landscape fragmentation (Zhang et al., 2022). It is essential to assess the degree of cultivated land fragmentation using landscape pattern indices and establish a reasonable cultivated land fragmentation evaluation model (Chen et al., 2012).

In this study, 164 street-level units with cultivated land in Beijing in 2017 and 163 street-level units with cultivated land in Beijing in 2022 were selected as samples. Then the scale class, shape class, agglomeration class and comprehensive fragmentation index of cultivated land in each research unit were calculated This evaluation model helps analyse the distribution of cultivated land patches and provides a quantitative and qualitative description of their shape. The 12 landscape pattern indices selected have different units, which could significantly impact the results. To standardize the indices and eliminate scale differences' influence, each index needs to be dimensionless. In the CRITIC weighting method (Liu et al., 2019), both forward and inverse normalization processes are usually used. When the evaluation indicator to be processed is a positive indicator, the formula for the normalization process is:

$$x'_{ij} = \frac{x_j - x_{min}}{x_{max} - x_{min}} \quad (2)$$

When the indicator to be evaluated is a negative indicator, the formula for the reversalization process is:

$$x'_{ij} = \frac{x_{max} - x_j}{x_{max} - x_{min}} \quad (3)$$

Where x'_{ij}=the dimensionless value
x_{ij}=the original value of the indicator
x_{imin}, x_{imax} = the minimum and maximum values in the sample respectively

The categories and indicator attributes of each indicator are shown in the table below.

Class	Name	Stats
Scale class	NP	+
	PD	+
	LPI	-
	AREA_AM	-
	LSI	+
shape class	SHAPE_AM	+
	ED	+
	FRAC_MN	+
	AI	-
Aggregation class	CLUMPY	-
	DIVISION	+
	CONTAG	-

Table 4. Classification of index of fragmentation evaluation system.

To reflect the contribution of different indicators to cultivated land fragmentation, it is necessary to assign weights to each indicator. This study chose the CRITIC weighting method to determine these weights. The intensity of comparison among indicators is expressed through the standard deviation: a larger standard deviation implies greater variability of an indicator across different units, indicating a significant difference in values between regions. Indicators with substantial differences should be assigned higher weights to highlight this discrepancy. Weights for each index were calculated accordingly (Zhao and Feng, 2024). Subsequently, the comprehensive index method was employed to compute the degree of cultivated land fragmentation for each street-level unit in Beijing, with the formula:

$$R_i = \sum_{j=1}^{n} p_{ij} \times w_j \quad (4)$$

Where R_i = the comprehensive fragmentation index of cultivated land in the ith evaluation unit

p_{ij} = the score of the jth indicator in the ith evaluation unit

w_j is the weight of the jth indicator.

Classification is carried out using the natural breakpoint method, identifying suitable breakpoints and categorizing them into graded levels. The degree of cultivated land fragmentation is then classified into five zones: very low value, low value, medium value, high value, and very high value, based on the graded results.

4. Experimental results and analysis

4.1 Cultivated land extraction results

The cultivated land patches of Beijing in 2017 and 2022 extracted by the trained model are depicted below. Overall, cultivated land in Beijing is primarily concentrated in the flat plains of the southeast, while sparse and fragmented patches of cultivated land are found scattered in the mountainous regions of the northwest, and urban construction areas have virtually no cultivated land. The model can extract the cultivated land more completely in the plain area with flat topography, intact plots and large cultivated land area, with fewer omissions.

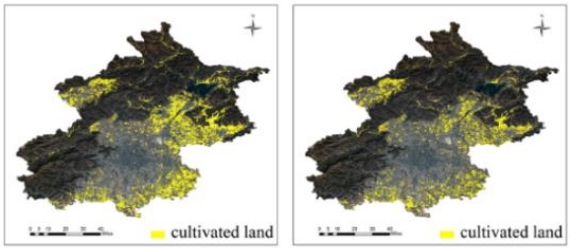

Figure 3. Results of cultivated land extraction in Beijing: (a) in 2017;(b) in 2022.

It also effectively identifies cultivated land devoid of vegetation cover and land cultivated during various crop growth stages. The training model's parameter configuration assigns a weight ratio of 4:1, with a higher weight assigned to cultivated land and a lower weight to non-cultivated land. This adjustment mitigates issues related to sample class imbalance during model learning, consequently enhancing its interpretive capabilities.

Figure 4. Results from cultivated land in plain area and adjacent to city.

Figure 5. Results of cultivated land extraction: (a) adjacent roads; (b) Hilly areas with gentle terrain.

The model can effectively identify the boundaries of cultivated land adjacent to roads and other land uses such as urban areas. It also performs well in mixed areas where cultivated land has irregular shapes, is fragmented, or has low differentiation, as well as in regions with complex topography, extracting irregularly shaped and sporadically distributed cultivated land in mountainous areas.

However, the model sometimes misclassifies small amounts of construction land, forest land, and grassland as cultivated land. The features of these land types sometimes closely resemble those of cultivated land without vegetation cover, making them difficult to distinguish even through manual visual inspection. Consequently, the model also performs poorly in recognizing cultivated land that is challenging to identify visually in the images.

To quantitatively evaluate the extraction results, a test area was randomly selected from each of the 2017 and 2022 images of cultivated land in Beijing. The extraction results were superimposed on manually labeled maps, which were evaluated by a series of comprehensive evaluation metrics, including

Overall Accuracy (OA), Producer Accuracy (PA), User Accuracy (UA), and Kappa Coefficient. The calculated Overall Accuracy (OA) is 0.9208, the Producer Accuracy (PA) is 0.1709, User Accuracy (UA) is 0.1702 and Kappa Coefficient (K) is 0.8358. The confusion matrix is shown below.

	The predicted result is non-cultivated land/ km²	Predicted cultivated land/ km²
Sample non-cultivated land	499.6919	34.4481
Sample cultivated land	36.5333	325.3267

Table 5. Confusion matrix of cultivated land extraction results.

4.2 Kernel density analysis

Using the data management tool of ArcGIS, the extracted cultivated land vectors were converted from surface elements to point elements. The kernel density analysis tool was then used to obtain the kernel density distribution maps for the distribution of cultivated land in Beijing for the years 2017 and 2022.In general, from 2017 to 2022, the extent of areas with very high kernel density values for cultivated land in Beijing has significantly reduced, and the distribution shows a trend of decentralization.

The spatial distribution pattern of cultivated land in Beijing is characterized by "polycentricity", with a linear distribution pattern along the southeastern part of the city. There is almost no cultivated land in the high altitude and steep mountainous areas. Low-nuclear-density areas are mainly located in the downtown area of Beijing and mountainous regions, which are unsuitable for agricultural development due to their political, economic, and natural conditions. These areas are highly developed, with less cultivated land. The distribution is shown in the figure below.

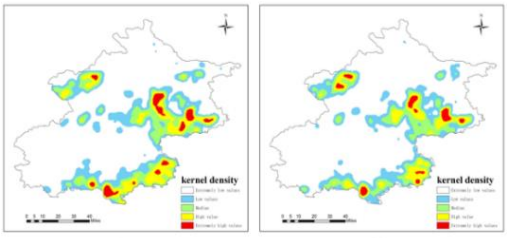

(a) (b)

Figure 6. Nuclear density analysis results: (a) 2017; (b) 2022.

New urban development zones located in the plains, such as Fangshan District and Daxing District, are important areas for undertaking appropriate functions of the central city and for population dispersal, and the area of cultivated land has been reduced. Meanwhile, in order to strictly implement the cultivated land protection system and ensure the bottom line of cultivated land size, cultivated land in ecological protection zones, such as Shunyi and Pinggu districts, is widely distributed and maintained in good condition.

4.3 Analysis of Changes in Cultivated land Utilization

The topography of Beijing consists mainly of plains, mountains and hills. The slopes in the mountainous and hilly areas are steep and prone to soil erosion, which is not conducive to cultivation of cultivated land. Using 90-meter DEM data in Beijing and Arcgis spatial analysis tool to calculate the slopes, the slopes were categorized into three ranges: 0-5°, 6-15° and 16-25°. Analysis results indicate that from 2017 to 2022, the area of cultivated land on slopes between 15-25° decreased the most significantly. These areas have poor soil and water conservation, requiring comprehensive measures to prevent soil and water erosion.

	≤5°/km²	6~15°/km²	16~25°/km²
2017	899.70	96.70	24.13
2022	727.30	71.53	11.63
Area of change	-172.40	-25.17	-12.50

Table 6. Changes in cultivated land under different slopes.

Water resource is an important factor to ensure the quality of cultivated land, and the soil quality of cultivated land near water systems is typically better and suitable for crop cultivation. Based on Beijing's specific conditions, a 500-meter buffer zone from cultivated land to water system was established to buffer the water system data in Beijing. This buffer layer was overlaid with the cultivated land in Beijing to analyze changes in cultivated land influenced by water systems from 2017 to 2022.

	In-stream buffer/ km²	Out of stream buffer/ km²	Research area/ km²
2017	396.94	623.59	1020.53
2022	303.56	506.90	810.46
Area of change	-93.38	-116.69	-210.07

Table 7. Changes in cultivated land under the influence of stream.

During this period, the area of cultivated land within the 500-meter buffer zone of the water system was reduced by a smaller amount, with the total area reduced by 93.38 km², while the area of cultivated land outside the buffer zone decreased by 116.69 km².The road network in Beijing is intricate. The expansion of this road network, along with road construction, impacts the ecological environment, leading to a reduction in cultivated land area and an increase in fragmentation.

According to the actual situation of Beijing, a 100-meter buffer zone from cultivated land to road was set up, and the buffer layer was superimposed with cultivated land to obtain the change of cultivated land in Beijing from 2017 to 2022. Although the total area of cultivated land in Beijing has shown a downward trend, the decrease of cultivated land is more pronounced within 100 meters of roads. The area of cultivated land outside the road buffer zone decreased by 15.48% to 117.94 km². In contrast, the cultivated land in the buffer zone decreased by 35.67% equalling 92.13 km².

	Cultivated land distribution/ km²		
	Within road buffer zone	Off-road buffer	Research area
2017	258.78	761.75	1020.53
2022	166.65	643.81	810.46
Area of change	-92.13	-117.94	-210.07

Table 8. Changes in cultivated land under the influence of road.

4.4 Landscape pattern index and fragmentation analysis

The vector map spots of cultivated land were converted into 10m raster data by Arcgis conversion tool. The raster data was then imported into Fragstats, and the landscape pattern indices required for the study were calculated. The calculation results are shown in the table below:

Landscape pattern index at class scale	2017	2022
NP	4766	4673
PD	0.285	0.279
AI	91.239	89.494
LPI	0.237	0.031
LSI	87.109	83.095
AREA_AM	323.271	55.533
SHAPE_AM	2.297	1.603
CLUMPY	0.908	0.891
DIVISION	0.896	0.934

Table 9. Calculation results of landscape pattern index at class scale.

Landscape pattern index at landscape scale	2017	2022
ED	6.251	4.738
FRAC_MN	1.006	1.052
CONTAG	81.742	86.873

Table 10. Calculation results of landscape pattern index at landscape scale.

The calculation results indicate that from 2017 to 2022, LPI decreased significantly, indicating that the distribution of cultivated land patches is heavily influenced by human activities, probably due to the development of agricultural land such as urban expansion and road construction, which led to a more irregular shape of cultivated land. The notable decrease of AREA_AM also corroborated this situation, showing a significant reduction in the average area of cultivated land patches.

This indicates that the originally piece of continuous cultivated land was divided into many fragmented cultivated land patches due to human factors. The overall landscape pattern indices of cultivated land patches all indicate that cultivated land aggregation in Beijing is high, but is decreasing. The complexity of cultivated land shapes is increasing, and the increase in complexity is particularly pronounced relative to regular shapes of the same size.

Calculated weights for the indicators of the evaluation system for the degree of cultivated land fragmentation in Beijing in 2017 and 2022 are presented in the table below:

Class	Index	2017 index weights	2022 index weights
Scale	NP	40.35%	33.90%
	PD	25.02%	21.89%
	LPI	20.16%	20.58%
	AREA_AM	14.47%	23.63%
Shape	LSI	32.81%	28.88%
	SHAPE_AM	13.36%	13.11%
	ED	35.15%	39.79%
Aggregation	FRAC_MN	18.68%	18.22%
	DIVISION	19.38%	20.96%
	CLUMPY	12.58%	20.78%
	AI	17.31%	24.06%
	CONTAG	50.73%	34.20%
comprehensive	Aggregate	35.41%	31.45%
	Shape	32.44%	49.01%
	Scale	32.15%	19.55%

Table 11. Calculation results of the weights of each index in the evaluation system of cultivated land fragmentation in 2017 and 2022.

Based on the results of weight calculation, the size class, shape class, aggregation class and comprehensive class fragmentation of each street-level administrative unit in Beijing in 2017 and 2022 are determined, and the spatial distribution map of comprehensive class fragmentation is depicted in the following figure.

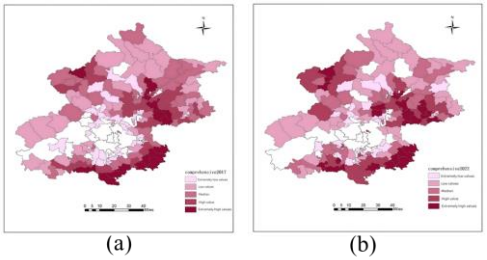

(a) (b)

Figure 7. Comprehensive spatial distribution map of fragmentation: (a) 2017; (b) 2022.

The spatial distribution map of cultivated land fragmentation in 2017 reveals that a total of 15 street-level units exhibit extremely high values of fragmentation. These areas are predominantly distributed in regions with gentle slopes in Mentougou, the southeastern part of Fangshan, Daxing and Tongzhou districts, as well as the plain areas in Miyun district. In these areas, cultivated land is more dispersed, displaying pronounced spatial clustering characteristics, and the shape of cultivated land patches appears irregular, as indicated by the shape class indicator.

By subtracting the integrated cultivated land fragmentation value in 2022 from that of 2017, we obtained the variation in integrated cultivated land fragmentation value from 2017 to 2022. From the results, it can be seen that, across Beijing, there are 46 street-level administrative units experienced an increase in the comprehensive fragmentation of cultivated land. These areas are mainly concentrated in the fringe areas near the main urban zones, such as Daxing and Haidian districts, as well as in the

mountainous areas like Miyun and Yanqing districts. Cultivated land near the main urban areas has become more severely fragmented due to the construction of roads and other infrastructure, the expansion of built-up areas, and the intervention of the other human activities. Mountainous areas, with their complex terrain and steep slopes, are unsuitable for extensive farming. Although less intervened by human activities, they lack the natural conditions for continuous large-scale crop cultivation, thus leading to cultivated land fragmentation to better adapt to the terrain and hydrological environment. The fragmentation of cultivated land in the rest of the region has decreased, probably due to the response to the national policy of cultivated land protection and the designation of cultivated land protection agglomeration areas, which has eased the fragmentation and fragmentation of cultivated land.

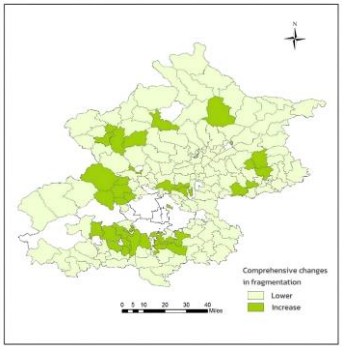

Figure 8. Spatial distribution of comprehensive fragmentation from 2017 to 2022.

5. Conclusion and outlook

In this paper, we conducted an exploratory research on cultivated land extraction using deep learning methods. We employed the HRNet deep learning network for model training, evaluated the training results, and completed the extraction of cultivated land in Beijing. To evaluate the accuracy of the model's extraction effect, a test area was selected, and the confusion matrix and Kappa coefficient were calculated. The Kappa coefficient is 0.8358, demonstrating the high accuracy of the extraction method. Furthermore, based on landscape pattern indices, we developed a cultivated land fragmentation evaluation system at the street level in Beijing. Considering the attributes and spatial patterns of Beijing's cultivated land, we selected 12 landscape pattern indices. We employed the CRITIC weight method to determine the weights of these indices, thereby constructing a comprehensive cultivated land fragmentation evaluation system. This approach extends the evaluation dimensions, making the analysis results more region-specific, scientific, and comprehensive.

Subsequently, the evaluation method can be continuously improved to better understand the current situation of Beijing's cultivated land from the perspective of cultivated land protection. This will help explore more targeted and effective cultivated land protection measures, thereby contributing to the process of sustainable development.

Acknowledgements

This work was supported by the National Natural Science Foundation of China (42201514).

References

Akhyar, A., Zulkifley, M.A., Lee, J., et al, 2024: Deep artificial intelligence applications for natural disaster management systems: A methodological review. *Ecological Indicators*, 163, 112067. doi.org/10.1016/j.ecolind.2024.112067.

Brabec, E., Smith, C., 2002: Agricultural Land Fragmentation: The Spatial Effects of Three Land Protection Strategies in the Eastern United States. *Landscape and Urban Planning*, 58, 255-268. doi.org/10.1016/S0169-2046(01)00225-0.

Cai, Y., Lin, H., Zhang, M., 2019: Mapping paddy rice by the object-based random forest method using time series Sentinel-1/ Sentinel-2 data. *Advances in Space Research*, 64. doi.org/10.1016/j.asr.2019.08.042.

Chen, H.Y., Zhu, D.L., Yun, W.J., et al, 2012: Analysis on cultivated land fragmentation and spatial agglomeration pattern in Jiaxing city. *Nongye Gongcheng Xuebao/Transactions of the Chinese Society of Agricultural Engineering*, 28, 235-242. doi.org/10.3969/j.issn.1002-6819.2012.04.039.

Chen, X., Xu, D., Fadelelseed, S., et al. 2019: Spatiotemporal Analysis and Control of Landscape Eco-Security at the Urban Fringe in Shrinking Resource Cities: A Case Study in Daqing, China. *International Journal of Environmental Research and Public Health*, 16, 4640. doi.org/10.3390/ijerph16234640.

Gong, C., Han, J., Lu, X., 2017, Remote Sensing Image Scene Classification: Benchmark and State of the Art. *Proceedings of the IEEE*, 105, 1865-1883. doi.org/10.1109/JPROC.2017.2675998.

Geng, S., Ma, M., Hu, X., et al, 2021: Multi-Scale Geographically Weighted Regression Modeling of Urban and Rural Construction Land Fragmentation–A Case Study of the Yangtze River Delta Region. *IEEE Access*, PP(99), 1-1. doi.org/10.1109/ACCESS.2021.3131329.

Huang, J., Zhu, Z., Huang, G., 2019: Multi-Stage HRNet: Multiple Stage High-Resolution Network for Human Pose Estimation. *ArXiv*, 1910.05901.doi.org/ arxiv-1910.05901.

Huang, Z.H., Du, X.J., Castillo, C.S.Z., et al. 2019: How does urbanization affect farmland protection? Evidence from China. *Resources Conservation and Recycling*, 145, 139-147. doi.org/10.1016/j.resconrec.2018.12.023.

Li, Y.S., Shi, T., Zhang, Y.J., et al. 2021: Learning deep semantic segmentation network under multiple weakly-supervised constraints for cross-domain remote sensing image semantic segmentation. *ISPRS Journal of Photogrammetry and Remote Sensing*, 175, 22-33. doi.org/10.1016/j.isprsjprs.2021.02.009

Liu, J., Jin, X.B., Xu, W.Y., et al. 2019: Influential factors and classification of cultivated land fragmentation, and implications for future land consolidation: A case study of Jiangsu Province in eastern China. *Land Use Policy*, 88, 104185. doi.org/10.1016/j.landusepol.2019.104185.

Liu, M.L., Liu, X.N., Wu, L., et al. 2021: Establishing forest resilience indicators in the hilly red soil region of southern China from vegetation greenness and landscape metrics using dense Landsat time series. *Ecological Indicators*, 121, 106985. doi.org/10.1016/j.ecolind.2020.106985.

Qiu, J.X., Wang, X.K., Lu, F., et al. 2021: The spatial pattern of landscape fragmentation and its relations with urbanization and socio-economic developments: a case study of Beijing. *Acta Ecologica Sinica*, 32, 2659-2669. doi.org/10.5846/stxb201104010426.

Tian, Y ., Shi, X.Y., 2024: Analysis of Dynamic Evolution and Driving Factors of Low-Carbon Utilization Efficiency of Cultivated Land in China. *Agriculture*, 14, 526. doi.org/10.3390/agriculture14040526.

Wahyudi, A., Liu, Y., Corcoran, J. 2018: Combining Landsat and landscape metrics to analyse large-scale urban land cover change: a case study in the Jakarta Metropolitan Area. *Journal of Spatial Science*, 64, 515–534. doi.org/10.1080/14498596.2018.1443849.

Yin, J., Wu, X.X., Shen, M.G, et al. 2019: Impact of urban greenspace spatial pattern on land surface temperature: a case study in Beijing metropolitan area, China. *Landscape Ecology*, 34, 2949–2961. doi.org/10.1007/s10980-019-00932-6.

Yin, H.B., Zhao, X.Y., 2024: Urban heat island analysis based on high resolution measurement data: A case study in Beijing. *Sustainable Cities and Society*, 106, 105389. doi.org/10.1016/j.scs.2024.105389.

Zhao, Y., Feng, Q., 2024: Identifying spatial and temporal dynamics and driving factors of cultivated land fragmentation in Shaanxi province. *Agricultural Systems*, 217, 103948. doi.org/10.1016/j.agsy.2024.103948.

Zhao, M.X., Nan, M., Yu, C.X., et al. 2023, SpineHRformer: A Transformer-Based Deep Learning Model for Automatic Spine Deformity Assessment with Prospective Validation. *Bioengineering*, 10, 1333. doi.org/10.3390/bioengineering10111333.

Zhang, J., Chen, M.Q., Huang, C., et al. Labor Endowment Cultivated Land Fragmentation and Ecological Farming Adoption Strategies among Farmers in Jiangxi Province, China. *Land*, 11, 679. doi.org/10.3390/land11050679.